

## AMTEC CLUSTERS FOR POWER GENERATION IN A CONCENTRATED SOLAR POWER PLANT

A. Onea<sup>1</sup>, N. Diez de los Rios Ramos<sup>1</sup>, W. Hering<sup>1</sup>,  
J.L. Palacios<sup>2</sup>, R. Stieglitz<sup>1</sup>

<sup>1</sup> Karlsruhe Institute of Technology,  
Institute for Neutron Physics and Reactor Technology,  
Hermann-von-Helmholtz Platz 1, 76344 Eggenstein-Leopoldshafen, Germany  
e-Mail: alexandru.onea@kit.edu

<sup>2</sup> University of Oldenburg, Ammerländer Heerstraße 114-118, 26129 Oldenburg

The present study reports a first estimation of the number of Alkali-Metal Thermal-to-Electric Converter (AMTEC) cells required for an AMTEC-Concentrated Solar Power (CSP) hybrid power plant in the 100 MWth class envisaged in [3]. The materials for the electrodes are also discussed and the best candidates are identified. Furthermore, numerical results obtained for the structural analysis of an experimental AMTEC cell developed at the Karlsruhe Institute of Technology (KIT) are reported.

**Introduction.** Promoted by the changes in the German energy policy (called “Energiewende”) “green” technologies, such as geothermal, wind and solar power, have received increased interest. Of high priority are renewable energy sources with load balancing capabilities such as concentrated solar power. To become an interesting option for industry, the efficiency of the thermal plant has to be increased. In this context, the Alkali-Metal Thermal-to-Electric Converter technology is considered as an option for a topping system for CSP [1]. Together with a thermal energy storage (TES) device it represents a promising solution for the extension of the global efficiency and of the total electrical output of a thermal power plant. AMTEC devices are based on the unique property of  $\beta$ -alumina ceramics, such as  $\beta''$ -alumina solid electrolyte (BASE), to allow the transport of alkaline (sodium) ions, while having a high electric resistivity. On the anode side of an AMTEC cell characterized by high temperature ( $\sim 800^\circ\text{C}$ ) and relative high pressure ( $\sim 10^5$  Pa), the sodium ionizes, with ions being transported through the BASE and electrons directed towards an external load to produce electricity. On the cathode side of the cell characterized by lower temperature ( $250 - 500^\circ\text{C}$ ) and lower pressure ( $10 - 100$  Pa), the ions recombine with the electrons to form neutral sodium molecules in vapor state which condense at cold side and are circulated back to the anode side, to close the cycle (see Heinzl *et al.* [2]).

Sodium has been recently identified as the best heat transfer fluid for thermal power plants, delivering the largest electrical energy to the grid and achieving the largest efficiency of the ideal delivered electricity, according to Liu *et al.* [3]. Considering the same input thermal energy, liquid sodium has the highest average heat transfer rate compared with compressed air at 10 bar, supercritical  $\text{CO}_2$  at 100 bar, steam at 10 bar and molten salt. This result is attributable to its high thermal conductivity.

Recently a concept of using liquid metals such as sodium for a hybrid thermal solar plant using AMTEC technology has been proposed by Hering *et al.* [1].

As an alternative for delivering the electrical base load, this new concept envisages the use of a TES that will allow the continuous operation of the facility during night and will also compensate short time heat fluctuations that can occur during day operation. Furthermore, the mid-day maximum in the thermal

energy can be used by employing the AMTEC technology as an add-on system for direct generation of electricity. This variant allows the use of conventional materials (e.g. stainless steel 1.4571) for the low temperature region ( $< 550^{\circ}\text{C}$ ), reducing therefore, the construction costs. At higher operating temperatures, the AMTEC modules will ensure the direct conversion of the thermal energy into electrical energy. The AMTEC cold side operates at temperatures  $< 500^{\circ}\text{C}$  and it is connected to the hot side of the TES. By this solution the “cold” sodium from the storage tank at  $\sim 200^{\circ}\text{C}$  is heated by the “waste” energy generated by the AMTEC devices. A concept design for a compact, small size solar thermal receiver using AMTEC converters has been proposed by Tanaka [4]. It is reported that the system conversion efficiency in maximum mode reaches 20% and generates  $\sim 12$  kWe, while in maximum output mode reaches 18% and generates almost 23 kWe.

**1. Overview of thermoelectrical converters for solar energy conversion.** Thermoelectrical (TE) devices that have the potential to be employed for the conversion of the solar energy into electricity are the converters based on the Seebeck effect, the thermionic converters, the AMTEC converters and the solar cells.

Heat engines based on the Seebeck effect that use solar energy for electricity production are known as solar thermoelectric generators (STEGs). In comparison to classical CSP systems, STEGs can operate at higher temperatures and do not require moving parts or working fluids, while having similar efficiencies of about 15%. An efficiency up to 15.9% is reported by Baranowski *et al.* [5] with present materials that exhibit a figure of merit  $Z_T = S^2\sigma T/\kappa = 1$ , where  $S$  denotes the Seebeck coefficient,  $\sigma$  [ $\Omega^{-1}\text{m}^{-1}$ ] represents the electrical conductivity,  $T$  is the temperature, and  $\kappa$  [ $\text{WK}^{-1}\text{m}^{-1}$ ] denotes the thermal conductivity. For improved materials ( $Z_T = 2$ ) and increased operating temperatures ( $1500^{\circ}\text{C}$ ), an efficiency of about 30% can be considered [5]. Conventional thermionic converters operate at temperatures exceeding  $1000^{\circ}\text{C}$ , and some applications include coupling to nuclear power units for electricity production in space. Even at these high temperatures, operating efficiencies only up to about 20% can be reached. Recently, the concept of photon-enhanced thermionic emission (PETE) for harvesting the solar energy has been proposed [6] by combining the thermal and photovoltaic carrier excitation with the thermionic emission. In contrast to conventional thermionic converter, the electrodes are held at the same temperature while vacuum is applied between them, and the cathode is side-illuminated rather than front-illuminated [7]. The illumination of the cathode increases the electronic conduction band of the cathode and consequently the energy barrier of the electrons to vacuum is reduced, allowing, therefore, the emission of electrons at lower temperatures than conventional thermionic converters. One advantage of the new concept is the reported increased efficiency up to about 40% at about  $900^{\circ}\text{C}$ .

Theoretically, optimized AMTEC cells can reach efficiencies up to  $\sim 40\%$  [8], but in practice lower efficiencies of  $\sim 25\%$  [1, 15, 16, 17] have been reached. The decreased output power during long time operation is one drawback of the cell and it is mainly attributable to the chemical changes occurring in the electrolyte and in the electrodes. Nevertheless, the operation of an AMTEC module for more than 5 years without power loss is reported in [9]. Although no explanations are given by the authors for this achievement, it possibly confirms the existence of a critical current density below which no power loss occurs.

For comparison purposes, the solar cells are also considered since they belong also to the class of direct energy converters. For crystalline amorphous silicon solar cells, Panasonic [10] reported recently an efficiency of 25.6% for the HIT

Table 1. Overview of the main thermoelectrical converters for solar energy conversion.

Thermoelectric device	Main advantages	Disadvantages
Thermoelectric converter (Seebeck effect)	Appropriate for applications with high temperature ( $T > 200^\circ\text{C}$ ) and low power (few watts). No moving parts	Low efficiency ( $<15\%$ ), high costs, high output resistance. Semiconductors for high temperatures ( $T > 1000^\circ\text{C}$ )
Thermionic converter (TC)	Coupling to nuclear power units for space missions. Applications using solar energy (PETE concept) can deliver $\sim 40\%$ efficiency at $\sim 900^\circ\text{C}$	Conventional TC's have low efficiency ( $<20\%$ ). Conventional TC require high thermal energy ( $T > 1500^\circ\text{C}$ )
AMTEC converters	Thermodynamically appropriate for CSP systems with Na as a heat carrier. Flexible thermal energy input. Robust, silent, reduced maintenance	Moderate efficiency (lower than theoretical value). Power loss during long time operation
Solar cells	Industrial production. Low thermal energy required. Low maintenance	Rather low efficiency ( $<20\%$ ). Expensive manufacturing and materials. Disposal of rare elements

(Heterojunction with Intrinsic Thin layer) solar cell. While all-single junction cells have theoretical efficiency of up to 31%, the multi-junction cells can reach larger efficiencies. The highest efficiency achieved presently is about 47% [11, 12], for a four-junction solar cells that use semiconductor materials stacked on top of each other. The drawback of the multi-junction cells is that their price is significantly larger than for the commercially available cells, which have efficiencies  $< 20\%$ .

The main advantages and drawbacks of the technologies discussed above are summarized in Table 1.

## 2. Preliminary layout of the AMTEC system for CSP .

2.1. *Assessment relative to the sizing of an AMTEC cluster.* For the hybrid system AMTEC and Concentrating Solar Power (A&CP), the AMTEC system envisaged should be dimensioned in the range 1–10 MWe, for a total system thermal output of about 100 MWth. The ratio can be optimized to meet the needs of the projected power plant. The yearly averaged thermal energy potentially available for AMTEC system, which is location dependent, should be correlated with the size of the base plant, receiver, and to the TES in order to properly dimension the AMTEC system.

For an AMTEC cell, the power vs. amperage curve has an inverted U-shape, defining therefore the voltage and amperage at the peak of the profile for maximal electrical power. Typically the maximum power density has been compared in the literature. Underwood *et al.* [13] proposed that the comparison should be made in terms of the AMTEC figure of merit  $Z_A = P_m/P_t$ , defined as the ratio of the measured maximum power density  $P_m = V_m I_m/A_e$ , where  $V_m$  is the applied voltage at maximum power,  $I_m$  is the total measured current at maximum power,  $A_e$  is the area of the electrode, to the theoretical maximum power density  $P_t$ . The theoretical maximum power [13] is the maximum power density produced minus

the losses due to resistances in the electrolyte, in the BASE/electrode contact and in the current feedthroughs. For the preliminary layout of the AMTEC system, the focus is on the maximum power density  $P_m$  that can be achieved by different configurations. Consideration of the figure of merit for a preliminary layout is still premature at this stage. A rough estimation of the number of BASE elements coated with electrodes for the output power required is performed in this study.

Although not the optimal design for an AMTEC cell, for the purpose of this study, a reference configuration cell is considered consisting of a single side closed cylinder with a surface of  $30 \times 200 \text{ mm}^2$  (diameter  $\times$  length) completely covered by a structured electrode. In order to determine the total electric power delivered, the best experimental results reported at maximal power for molybdenum (Mo) [1, 14], titanium nitride (TiN) [9, 16], titanium diboride (TiB<sub>2</sub>) [15], niobium nitride (NbN) [25], titanium carbide (TiC) [26] and rhodium tungsten (RhW) electrodes [17] have been linearly extrapolated for the AMTEC geometry considered, as displayed in Table 2. For all sets of data, the current density was kept constant, and the area of the electrode was extrapolated to the reference area.

For long time operation of the AMTEC system, the power loss has to be taken into account, in order to eliminate it from the design phase by appropriately setting the AMTEC operating parameters. Richman and Tennenhouse [18] report critical values for the current density below which no power loss occurs, e.g., a BASE containing 0.25 wt.% LiO<sub>2</sub> can be charged up to a current density of 1 A/cm<sup>2</sup> before power loss can occur. Nevertheless, this criterion has been reported for a low operational temperature of 300°C and a short operation time. Therefore, further experimental research is needed to validate the critical current density, which depends on the BASE chemical composition, for higher temperatures and for longer test periods that are relevant to AMTEC conditions.

The power dependence on the number of BASE elements is displayed in Fig. 1. The output electrical power determined is very sensitive to the operating characteristics of the cell. Beside the current density and operating temperature, many other issues, such as BASE and electrode thicknesses, electrode grain sizes, resistances of the current collector, current lead etc. have to be taken into account

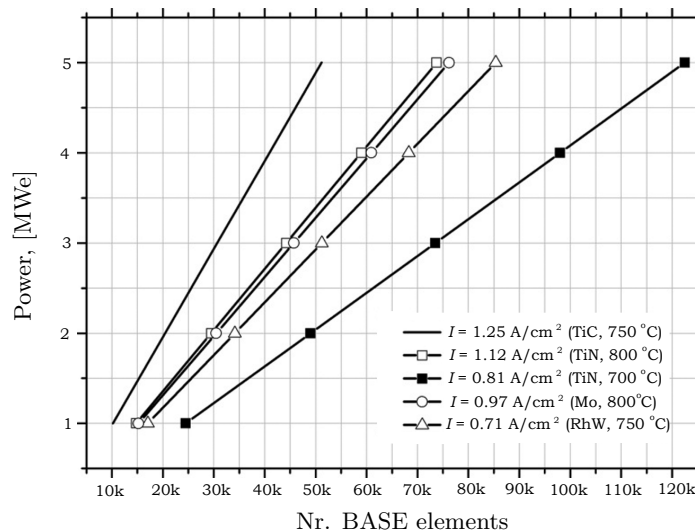


Fig. 1. Total electric power versus required BASE elements.

Table 2. Number of required BASE elements for 1 MWe function of electrode materials, temperature, and current density (extrapolated on the reference configuration).

Electrode	Mo	Mo	TiB <sub>2</sub>	TiB <sub>2</sub>	TiB <sub>2</sub>	NbN	TiC	RhW	TiN	TiN	TiN	TiN
Temperature [°C]	736	800	700	800	800	800	750	750	700	700	800	850
Current density [A/cm <sup>2</sup> ]	0.55	0.97	0.5	0.6	0.65	0.65	1.25	0.71	0.81	0.81	1.12	1.25
Voltage [V]	0.28	0.35	0.33	0.40	0.55	0.55	0.42	0.44	0.27	0.27	0.32	0.37
Electrode area [m <sup>2</sup> ] for $P_m = 1$ MW	638	287	612	421	280	280	193	322	462	462	278	219
Nr. BASE elements for $P_m = 1$ MW	33870	15239	32480	22337	14839	14839	10228	17074	24498	24498	14750	11598
$P_m/A_e$ [W/m <sup>2</sup> ]	1566	3481	1633	2375	3575	3575	5187	3107	2166	2166	3597	4574
Thickness electrode cathode side [μm]	1	1	2	2	6	6	5	~1	~32.5	~32.5	~32.5	~32.5
Mass electrodes [kg]	6.6	3.0	5.6	3.8	14.2	14.2	4.8	5.8	81.6	81.6	49.1	38.6
Data source	[1]	[14]	[6]	[6]	[25]	[25]	[26]	[17]	[16]	[16]	[16]	[16]

and correlated to achieve a robust AMTEC performance able to deliver a large amount of electrical energy without power loss. Kato *et al.* [26] reported one of the best electrical performances using TiC electrodes. At 750°C (current density 1.25 A/cm<sup>2</sup>), an electric output in the range of 1 MWe can be realized with approximately 10200 BASE elements coated, while at 800°C it can be roughly estimated from their data that a current density of ~1.5 A/cm<sup>2</sup> is achievable (0.75 W/cm<sup>2</sup>) and a power of 1 MWe can be generated using ~7090 BASE elements. AMTEC modules using Mo, TiN, NbN, RhW electrodes operated at 800°C can deliver 1 MWe using ~15000 cells. A much larger electrical output would impose significant raise in costs due to the increase in the number of BASE elements and is at least for the moment not realistic. The power loss that occurs when operating at high current density is one of the main open issues here and has to be further investigated. The long time operation of an AMTEC module without power loss reported in [9] can possibly be explained by the fact that the device was operated below the critical current density, taking into account the electrical parameters reported, i.e. very low voltage and amperage. Nevertheless, at larger electrical output, a very large number of BASE elements is required (see Table 2). Therefore, the task of identifying and increasing the critical current density above which power loss can occur has to be further pursued. Increasing the operating temperature would lead also to a larger electrical output, nevertheless appropriate materials have to be considered and the number of heliostats should be increased, both measures implying an increased manufacturing cost.

With the present technology, an electrical output of up to ~2 MWe can be achieved with ~30 000 BASE elements at 750–800°C (see Fig. 1) at a current density of about 1 A/cm<sup>2</sup>. Operated at larger temperature and increased current density, the same power could be achieved with fewer BASE elements. Nevertheless, in this case, it has to be ensured that the power loss remains at acceptable levels. The selling cost of 30000 BASE elements is roughly estimated in the moment at ~2.5 million EUR. For the A&CP plant, the aimed size of the AMTEC cluster is presently estimated to ~30,000 BASE elements, taking into account the electrical output that can be delivered, the costs and the constructive solutions. To obtain the balanced optimum between the maximum electric power delivered and constant performances during long-time usage, further studies have to be performed for a better estimation of the electrical power, taking into consideration also other AMTEC specific issues such as the small electrode effect.

*2.2. Discussion of electrode materials.* The proposed A& CP plant operates in the base mode below 500–550°C, while the AMTEC modules are switched on when thermal peak loads occur (during mid-day). At the moment, the maximum temperature for the operation of the AMTEC cluster is conservatively estimated to about 800–850°C, taking into account a maximum temperature of ~900°C at the receiver [3]. Although operating at a larger temperature would enhance the output electrical power, increased manufacturing costs due to the need of adequate steels have to be also deemed. The maximum operational time of the AMTEC modules required for the A&CP plant is conservatively estimated at ~7 years (60 000 hours).

The main requirements related to the electrodes are good electrical conductivity, good mechanical bonding to the BASE and a similar coefficient of thermal expansion with the BASE, chemically inert against sodium, and good permeability to sodium vapour. Electrodes are characterized by the charge exchange current coefficient  $B = j_0(T^{0.5}P^{-1})$ , where  $j_0$  is the exchange current,  $T$  the electrode temperature and  $P$  the pressure, and by the electrode vapour pressure loss factor  $G$ , which characterizes the capacity of sodium to travel through the electrode

towards the low pressure side. A high  $B$  value would imply a high net electrochemical potential generated across the BASE. Smaller  $G$  values imply a lower vapour pressure on the cathode and, hence, a higher electrochemical potential across the BASE.

The materials considered as candidates for electrodes, as well as some of the most relevant parameters are summarized in Table 3. For comparison, the BASE has typically a coefficient of thermal expansion of  $\sim 7.2 \times 10^{-6} \text{ K}^{-1}$  at  $25^\circ\text{C}$ .

The electrodes are responsible for about 20% of power loss in an AMTEC device [19]. Their main mechanism of power loss is the growth of grains, as the electrodes sinter with increasing temperature. As electrodes sinter, the grains coalesce and form larger grains, decreasing, therefore, the electrode transmission space and consequently the exchange current.

Ryan *et al.* [20] developed a model based on the grain growth mechanism for the power deterioration occurring in the electrodes. Considering a maximum operating period of 60 000 hours, the TiN electrodes can be operated up to a temperature of  $792^\circ\text{C}$ , while Mo electrodes can be operated up to temperatures of  $804^\circ\text{C}$  and still maintain 90% of their power. For this rather “short” operational time, RhW electrodes can be operated up to  $977^\circ\text{C}$  and still maintain more than 90% of their power.

Although molybdenum has rather good electrical performances with an acceptable power loss if the temperature is kept below  $800^\circ\text{C}$ , its main disadvantage is its reactive character with sodium, leading to the formation of sodium-molybdate ( $\text{Na}_2\text{MoO}_4$ ) in the electrode [21].  $\text{Na}_2\text{MoO}_4$  enhances the sodium transport due to ionic conduction up to its melting point ( $687^\circ\text{C}$ ). However, the performances degrade in time due to the evaporation of  $\text{Na}_2\text{MoO}_4$ . Under AMTEC relevant operating conditions (low sodium pressure and low activity),  $\text{Na}_2\text{MoO}_4$  can slowly corrode Mo and lead to the formation of  $\text{MoO}_2$  and Na. The reaction can reverse at increased sodium activity and operating temperature.

Titanium nitride electrodes exhibit generally lower electrical performances as Mo (smaller  $B$ , larger  $G$ ) and, although being chemically more stable than Mo, they exhibit significant power loss at rather low temperatures of less than  $\sim 800^\circ\text{C}$ . The latter characteristic decreases the chances of TiN for further consideration in an A&CP plant.

Ceramic electrodes such as  $\text{TiB}_2$ , TiC and NbN have many properties that make them interesting for application in A&CP (slow degradation, chemically inert vs. sodium). Though TiC and NbN have a rather large electrical resistivity, large power densities are reported in the literature (see Table 2). For TiC, one of the main reasons for the large power delivered is the fine particle size ( $< 0.1 \mu\text{m}$ ) used that ensured a long triple-phase boundary [26]. As drawbacks, NbN has a larger expansion coefficient than BASE and there is a rather reduced long-time operating experience with these electrodes. To the authors knowledge, no studies of the grain growth mechanism for these electrodes are reported in the literature. Nevertheless, it should be noted that ceramic electrodes should exhibit a slower grain growth compared to metallic electrodes, also due to their high melting point. Considering their electrical performances, TiC electrodes are appropriate candidates for usage in an AMTEC cluster in an A&CP plant, being able to deliver a large power density.  $\text{TiB}_2$  exhibits also excellent properties as well (low electrical resistivity, large  $B$ , small  $G$ , chemically inert in Na, similar expansion coefficient with BASE) and has good potential for the usage in an A&CP plant. Lanthanum hexaboride ( $\text{LaB}_6$ ) exhibits a good electrical conductivity with a peak power density of  $\sim 5400 \text{ W/m}^2$  and a good chemical stability in Na environment at the AMTEC relevant operating temperature [27]. However, no long-time studies

Table 3. Overview of candidate electrodes for AMTEC clusters.

Electrode	Electrical resistivity (25°C) $10^{-8} \Omega\text{m}$	Electrical resistivity (800°C) $10^{-8} \Omega\text{m}$	Melting point °C	Coeff. of therm. exp. (25°C) $10^{-6} \text{K}^{-1}$	$B$ $\text{AK}^{1/2} \text{Pa}\cdot\text{m}^2$	$G$	Remarks
Mo	5.5	26.1	2623	5.2	$\sim 400$		Rapid grain growth $> 827^\circ\text{C}$ . Long time operation: reaction with Na
TiN	$\sim 37$		2930	9.4	120	50	Reduced performances vs. Mo. Chemically inert vs. sodium and BASE[23]. Large power loss
TiC	$\sim 150$		3160	7.4			Chemically inert vs. sodium and BASE[23]. High electrical performances. No long-time experience
TiB <sub>2</sub>	20.4	47	3230	7.2	$\infty$	5	Better performances as Mo. Chemically inert vs. sodium[15]. No long-time experience
NbN	137		2573	10.1	407[25]	5[25]	Chemically inert vs. sodium and BASE[23]. No long-time experience
LaB <sub>6</sub>	$\sim 6.5$		2530	7.6			Chemically inert vs. sodium and BASE[27]. No long-time experience
RhW	41.3(Rh-6%W)	56.7(Rh-6%W)	W: 3422 ; Rh: 1964	W: 4.2 ; Rh: 8.4	90-110[20]	10-25[20]	Low power loss. Chemically stable. Rh extremely expensive
PtW	$\sim 65$	79	Pt: 1768	Pt: 9	$\sim 50$ [22]		Lifetime estimated up to $\sim 7$ yr. Chemical interaction with Mn from stainless steel[22]. Pt extremely expensive
Metal/oxide[16],[24]					90-110[24]	10[24]	Low power loss. Chemically stable

have been reported in the literature and its mechanism of power loss has not yet been reported either.

Tungsten rhodium electrodes have received increased interest in the recent period due to their good electrical performances (large  $B$ , small  $G$ , balanced power loss even at higher temperatures) and to their chemically inert behaviour against sodium. Nevertheless, they are also very expensive, and this aspect makes their usage questionable. Furthermore, larger power loss has been observed when the electrodes are based on Ni grids [22].

The platinum tungsten electrodes coupled to Mo grids exhibit a larger power density than RhW. However, besides their high costs and a rather low  $B$  coefficient, contamination with manganese from stainless steel casing was observed [22]. The predicted lifetime of PtW is significantly shorter than for RhW because Pt sinters more rapidly, and it is estimated to vary between 4 to 7 years, below the lifetime needed for an A&CP plant.

Recently, mixed metal/oxide (Mo or TiN with  $\text{TiO}_2$ ) electrodes have been proposed [16, 24] with the aim of enhancing both the ionic and electronic conductivity of the electrode. Although theoretically such electrodes should simultaneously enhance both the transport of  $\text{Na}^+$  and  $e^-$ , the results reported up to now show that the power obtained is slightly smaller than the one obtained for TiN electrodes [16]. Nevertheless, another advantage of the metal/oxide electrodes is that in comparison to RhW electrodes, they are inexpensive.

**3. AMTEC test facilities at KIT.** The experimental investigations and development of AMTEC cells have been recently restarted at KIT in the frame of two research projects, the Helmholtz alliance on LIquid Metal TECHnology (LIMTECH) and Helmholtz Energy Materials Characterization Platform (HEMCP). The experimental program is focused on short term tests and long term tests of AMTEC cells, as well as on tests of innovative materials for AMTEC cells in hot sodium environment. The short term tests are planned to start by the end of 2015 in the Amtec TEst FAcility (ATEFA) at KIT. A detailed description of the facility and of the research projects is given in [28, 29]. Long term tests are planned in parallel in another facility presently at the beginning of the construction phase at KIT. The experimental test campaign planned in the ATEFA facility is focused on AMTEC key issues, such as the tests of BASE ceramics, electrode materials, and stability of ceramic-metal interfaces.

**4. Structural analysis of the AMTEC test cell.** One of the critical issues related to an AMTEC cell is the BASE-metal interface. During operation, the BASE expands due to a thermal gradient that can reach up to several hundred °C. Since the BASE is connected to a metallic part, the BASE-metal interface is severely stressed by the thermal and mechanical stresses induced in this region. Many authors, including Heinzl *et al.* [1], report the crack of the BASE and suggest that the demanding operating conditions (high temperature, large temperature gradient across the BASE) induce severe stresses in the BASE that lead to its failure. Unfortunately, just a few studies can be found in the literature regarding the stress distribution in an AMTEC cell. These aspects motivated the structural analysis of the AMTEC test cell developed at KIT. The numerical analysis has been performed using the ANSYS V14.5 software. The cross-section of the cell is displayed in Fig. 2a To decrease the computational time, the numerical model considers only a 1/8 slice of the cell, with symmetry conditions applied on the lateral sides.

For the test cell, the BASE is connected to a metallic tube through a transition piece made of niobium (Nb). In the model, nickel has been considered for the welds of the transition piece.

The numerical model for the stationary state considers the steady-state thermal block for the determination of the temperature distribution and two steady state structural blocks, one for the entire cell and a sub-model for a finer discretization of the steel-Nb-BASE region. A grid study has been performed for each analysis block and grid-independent results have been obtained as follows: for the thermal block, constant temperature profiles were obtained with a grid of  $\sim 0.13 \times 10^6$  nodes; for the global structural block, a structural error of  $\sim 0.25 \times 10^{-5}$  mJ was obtained for a grid consisting of  $\sim 0.8 \times 10^6$  nodes, while for the sub-model, a structural error of  $\sim 0.8 \times 10^{-6}$  mJ was attained with a grid of  $\sim 2.3 \times 10^6$  nodes.

The structural analysis in the stationary state has been performed for the nominal operating conditions planned, considering the relevant parameters at their extreme range. The sodium temperature on the inner side of the BASE was set to  $1000^\circ\text{C}$  and the temperature of the condenser was set to  $250^\circ\text{C}$ , while a pressure gradient of  $0.2\text{ MPa}$  was considered across the BASE. For the welds, the maximum shear stress theory was considered to determine the safety factors. The maximum shear stress in the upper weld of the metal-Nb joint was  $9.1\text{ MPa}$ , corresponding to a safety factor of  $4.3$ , while the maximum shear stress in the bottom weld (Nb-BASE interface) was  $4.8\text{ MPa}$ , corresponding to a safety factor of  $8.2$ . The maximum von-Mises stress in the transition piece reached  $21.6\text{ MPa}$  (see Fig. 2b), which corresponds to a safety factor of  $6.4$ , considering the von-Mises effective stress theory. The maximum principal stress in the BASE was  $1.83\text{ MPa}$ , for which the safety factor was  $15$ , considering the Mohr-Coulomb theory for brittle

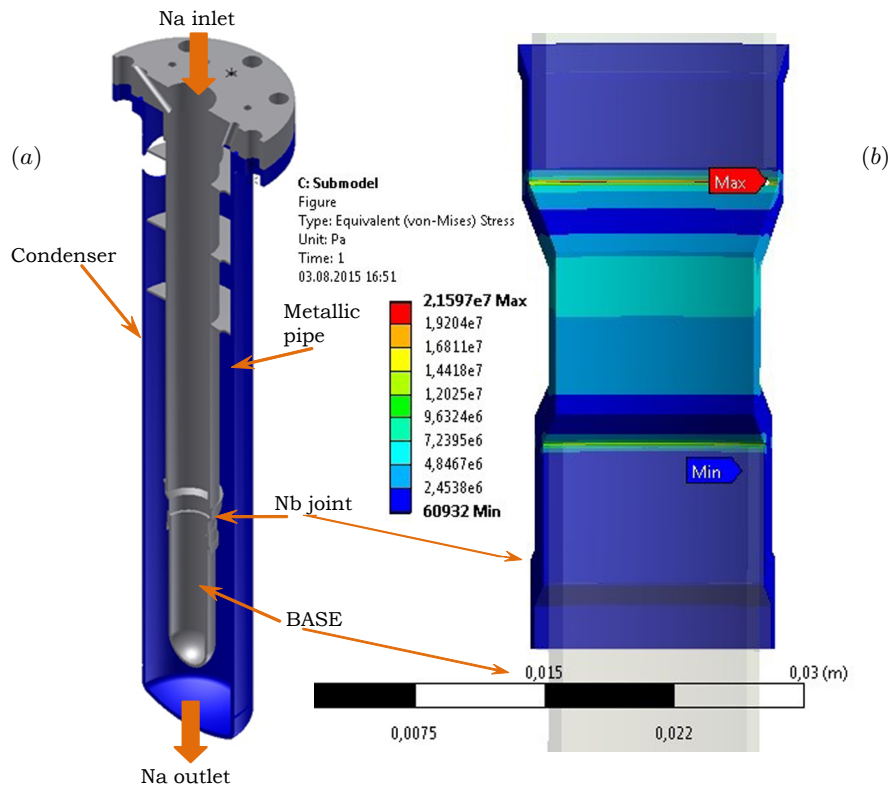


Fig. 2. (a) ANSYS model of the experimental AMTEC test cell. (b) Stress distribution in the transition piece at  $\Delta P = 0.2\text{ MPa}$  and  $\Delta T = 750^\circ\text{C}$ .

materials. Under these conditions, no material failure should occur in the test cell, since all safety factors determined are sufficiently large above unity. The upper welding between the transition piece and the metallic tube was determined to be the weakest component in the cell, due to the difference in the thermal expansion of the materials.

**5. Conclusions.** The use of an AMTEC cluster with  $\sim 30\,000$  BASE elements for a CSP plant coupled with a thermal storage tank can be achieved for an electrical output up to about 2 MWe if a robust AMTEC design can be attained able to operate on a long time basis at a current density of  $\sim 1\text{--}1.5\text{ A/cm}^2$  without a large power loss. Further investigations should be made to appropriately estimate the real electric power delivered by a cluster of AMTEC cells, considering in parallel the long time power behaviour. For the assessment of the economical feasibility of using AMTEC clusters in an A&CP plant, the next step is the evaluation of the averaged lifetime levelized cost of electricity (LCOE).

The main open issue concerning the ceramic is the investigation of the critical current density at the temperature range considered for an A&CP plant.

Regarding the materials for the electrodes, due to the rapid power loss that occurs at rather low temperatures, Mo and TiN electrodes are not optimal choices for AMTEC clusters in an A&CP plant. Furthermore, Mo reacts chemically with sodium, which is an undesired effect. Ceramic electrodes such as TiC, TiB<sub>2</sub>, and NbN have probably the best adequate properties for the use in an A&CP, exhibiting very good electrical performances, no chemical reaction with the BASE and sodium, and affordable costs. Nevertheless, appropriate investigations should be performed to determine their lifetime. Although Rh<sub>x</sub>W electrodes have very good electrical properties, their main drawback is related to their high cost. The metal/oxide electrodes are cheaper than Rh<sub>x</sub>W and have rather similar electrical performances. Therefore, they are good candidates as electrodes.

The AMTEC test cell has been numerically investigated with respect to its mechanical behaviour. The distribution of the stresses has revealed that the design made is safe and that no material failures should occur in the operating range considered. Further, the location of the highest stresses has been identified to be the region of the steel-Nb joint, due to the difference in thermal expansion coefficients.

**Acknowledgments.** The authors acknowledge hereby the financial support received from the Helmholtz alliance in the frame of the LIMTECH project.

## REFERENCES

- [1] W. HERING, R. STIEGLITZ, TH. WETZEL. Application of liquid metals for solar energy systems. *2nd European Energy Conference, Maastricht, Netherlands, European Physical Journal EPJ Web of Conferences*, vol. 33 (2012), pp. 03003.1–7.
- [2] V. HEINZEL, F. HUBER, W. PEPPLER, H. WILL. Technological tests with respect to the use of beta alumina in Alkali-Metal-Thermo-Electric converters (AMTEC). *Key Eng. Mat.*, vol. 59&60 (1991), pp. 381–394.
- [3] M. LIU, M. BELUSKO, S.N.H. TAY, F. BRUNO. Impact of the heat transfer fluid in a flat plate phase change thermal storage unit for concentrated solar power plants. *Solar Energy*, vol. 101 (2014), pp. 220–231.

- [4] K. TANAKA. Concept study of solar thermal receiver using alkali metal thermal to electric converter (AMTEC). *Current Applied Physics*, vol. 10 (2010), pp. S254–S256.
- [5] L.L. BARANOWSKI, G.J. SNYDER, E.S. TOBERER. Concentrated solar thermoelectric generators. *Energy Environ. Sci.*, vol. 5 (2012), p. 9055.
- [6] J.W. SCHWEDE, I. BARGATIN, D.C. RILEY *et al.* Photon-enhanced thermionic emission for solar concentrator systems. *Nature Materials*, vol. 9 (2010), pp. 762–767.
- [7] G. SEGEV, A. KRIBUS, Y. ROSENWAKS. High performance isothermal photo-thermionic solar converters. *Solar Energy Materials & Solar Cells*, vol. 113 (2013), pp. 114–123.
- [8] G.C. LEVY, T.K. HUNT, R.K. SIEVERS. AMTEC: current status and vision. *Proc. the Intersociety Energy Conversion Eng. Conference*, vol. 2 (1997), paper-ID 97536, pp. 1152–1155, .
- [9] T.K. HUNT, J.R. RASMUSSEN. Fractional watt AMTEC converter. *Proc. the Space Tech. Applic. Intern.* (Forum STAIF 2006), pp 567–572.
- [10] PANASONIC HIT SOLAR CELL ACHIEVES. World’s Highest Energy Conversion Efficiency of 25.6% at Research Level. <http://panasonic.co.jp/corp/news/official.data/data.dir/2014/04/en140410-4/en140410-4.html>.
- [11] F. DIMROTH, T.N. TIBBITS, P. BEUTEL *et al.* Development of high efficiency wafer bonded 4-junction solar cells for concentrator photovoltaic applications. *Proc. the 40th IEEE Photovoltaic Specialists Conference* (Denver, Colorado, 2014).
- [12] N. MILLER, P. PATEL, C. STRUEMPEL, C. KERESTES, D. AIKEN, P. SHARPS. Terrestrial concentrator four-junction inverted metamorphic solar cells with efficiency >45%. *Proc. the 40th IEEE Photovoltaic Specialists Conference* (Denver, Colorado, 2014).
- [13] M.L. UNDERWOOD, R.M. WILLIAMS, B. JEFFRIES-NAKAMURA, M.A. RYAN. A figure of merit for AMTEC electrodes. *Proc. the 26th Intersociety Energy Conversion Engineering Conference IECEC '91* (Boston, 1991), vol.5, pp. 475–480.
- [14] V. HEINZEL, F. HUBER, G. OCHS, W. PEPPLER, M. STEINBRÜCK, H. WILL. *Internal Report IRE4-1116-91* (1991).
- [15] Q. FANG, R. KNÖDLER. Porous TiB<sub>2</sub> electrodes for the alkali metal thermoelectric convertor. *J. Materials Science*, vol. 27 (1992), pp. 6725–6729.
- [16] R.W. FLETCHER, W. SCHWANK. Recent developments in mixed ionic and electronic conducting electrodes for the Alkali Metal Thermal Electric Converter (AMTEC). *Proc. the Space Tech. Applic. Intern. Forum STAIF 2003*, pp. 722–729.
- [17] J.-M. TOURNIER, M.S. EL-GENK. Design optimization of high-power, liquid anode AMTEC. *Proc. the Space Tech. Applic.* (Intern. Forum STAIF 2003), pp. 740–750.

- [18] R.H. RICHMAN, G.J. TENNENHOUSE. A model for degradation of ceramic electrolytes in Na-S batteries. *J. Am. Ceram. Soc.*, vol. 58 (1975), pp. 63–67.
- [19] M.A.K. LODHI, M.S. CHOWDHURY. The role of electrodes in power degradation of AMTEC: analysis and simulation. *J. Power Sources*, vol. 96 (2001), pp. 369–375.
- [20] M.A. RYAN, R.H. SHIELDS, R.H. CORTEZ, L. LARA, M.L. HOMER, R.M. WILLIAMS. Lifetimes of AMTEC electrodes: molybdenum, rhodium-tungsten, and titanium nitride. *Proc. the Space Techn. Appl.* (Int. Forum-2000), pp. 1377–1382
- [21] R.M. WILLIAMS, C.P. BANKSTON, S.K. KHANNA, T. COLE. Voltammetric studies of porous molybdenum electrodes for the Alkali Metal Thermoelectric Converter. *J. Electroch. Soc.: Electrochem. Sc. Tech.*, vol. 113 (1986), no. 11, pp. 2253–2257.
- [22] M.A. RYAN, B. JEFFRIES-NAKAMURA, R.M. WILLIAMS, M.L. UNDERWOOD, D. O’CONNOR, S. KIKKERT. Advances in materials and current collecting networks for AMTEC electrodes. *Proc. the 27th Intersociety Energy Conversion Eng. Conference* (1992), paper ID 929007, 3.7–3.12.
- [23] O. ASAKAMI, K. TSUCHIDA, H. TOGAWA, A. KATO. Material for the electrode of the alkali metal thermoelectric converter (AMTEC). *J. Mater. Sc. Letters*, vol. 8 (1989), pp. 1141–1143.
- [24] M.A. RYAN, R.M. WILLIAMS, L. LARA, B.G. FIEBIG, R.H. CORTEZ, A.K. KISOR, V.B. SHIELDS, M.L. HOMER. Advances in electrode materials for AMTEC. *Proc. the Space Techn. Appl.* (Int. Forum-2001), vol. 552, pp. 1088–1093.
- [25] A. KATO, K. TSUCHIDA, T. HASHIMOTO, H. NAKATA, T. NAGATA. Characteristics of ceramic electrode for AMTEC. *Proc. the 27th Intersociety Energy Conversion Eng. Conference* (1992), paper ID 929006, 3.1–3.6.
- [26] A. KATO, H. NAKATA, K. TSUCHIDA. Characteristics of ceramic electrode for AMTEC II. Structure of electrode and power density. *Proc. the 12th Int. Conference on Thermoelectrics* (1993), paper ID 93027, pp. 1.809–1.814.
- [27] K. TSUCHIDA, T. NAGATA, H. NAKATA, A. KATO. LaB<sub>6</sub> and TiB<sub>2</sub> electrodes for the alkali metal thermoelectric converter. *J. Mat. Science*, vol. 33 (1998), pp. 755–762.
- [28] A. ONEA, N. DIEZ DE LOS RIOS RAMOS, W. HERING, R. STIEGLITZ, P. MOSTER. Direct energy conversion using liquid metals. *European Physical Journal EPJ Web of Conferences*, vol. 79 (2014), pp. 03010.1–9.
- [29] N. DIEZ DE LOS RIOS RAMOS, A. ONEA, S. SCHERRER, A. WEISENBURGER, W. HERING. Direct energy conversion of heat to electricity using AMTEC. *5th International Youth Conference on Energy* (Pisa, Italy, 27–30.05.2015).

Received 30.10.2014